Self-Guided Quantum State Learning for Mixed States

Ahmad Farooq, Muhammad Asad Ullah, Syahri Ramadhani, Junaid ur Rehman, and Hyundong Shin

Department of Electronics and Information Convergence Engineering, Kyung Hee University, Korea

We provide an adaptive learning algorithm for tomography of general quantum states. Our proposal is based on the simultaneous perturbation stochastic approximation algorithm and is applicable on mixed qudit states. The salient features of our algorithm are efficient $(O\left(d^3\right))$ post-processing in the dimension d of the state, robustness against measurement and channel noise, and improved infidelity performance as compared to the contemporary adaptive state learning algorithms. A higher resilience against measurement noise makes our algorithm suitable for noisy intermediate-scale quantum applications.

1 Introduction

We require high-fidelity state preparation and its characterization for applications in quantum communication [1, 2], quantum computation [3, 4], and quantum metrology [5, 6]. Quantum state tomography is the task of inferring a quantum state from the statistics of measurements on multiple copies of the quantum system—which requires large computation and storage space. The tomography algorithm resorts often to least-square estimation [7], maximum likelihood estimation [8, 9], hedged maximum likelihood estimation [10], Bayesian mean estimation [11–14], and linear regression estimation [15, 16].

Some recent proposals for quantum state tomography include self-guided quantum tomography (SGQT), practical adaptive quantum tomography (PAQT), and state tomography through eigenstate extraction with neural networks [17–22]. SGQT employs a stochastic approximation optimization technique known as simultaneous perturbation stochastic approximation (SPSA) [23] to learn an unknown pure state. This online machine learning technique converges to the desired unknown state extremely fast and requires much fewer amount of space and time as compared to other known standard quantum tomography algorithms. Furthermore, it is robust to noise, which is a highly desirable property in near-term quantum devices. However, its restriction to pure states seriously limits its utility in general scenarios where we often encounter mixed quantum states. The PAQT algorithm aims to remove this limitation by generalizing it to the mixed states. It achieves this feat by applying Bayesian mean estimation on data generated by the SGQT [19]. The PAQT inherits the aforementioned desirable properties of the SGQT including efficiency in storage space and computation and robustness to noise.

In this paper, we propose a quantum state tomography algorithm, called the self-guided quantum state learning for mixed state, to estimate mixed quantum states of dimension d. The main ingredient of our algorithm is the observation that the SPSA algorithm converges to the eigenvector corresponding to the highest eigenvalue of a given unknown mixed

Hyundong Shin: hshin@khu.ac.kr, (corresponding author)

state. We perform the complete characterization of an unknown mixed state by iteratively invoking the SPSA on the intersection of nullspace of already obtained eigenvectors. After estimating all eigenvectors and eigenvalues, we employ the Gram-Schmidt process to generate an orthonormal spectrum of the unknown state. This procedure produces accurate estimates of the unknown state with efficient post-processing and superior robustness to noise as illustrated by the numerical examples. Importantly, if the unknown given quantum state is pure, our algorithm is equivalent to the SGQT algorithm. Thus, inheriting all the desirable properties of SGQT for the pure state tomography.

The remainder of this paper is organized as follows. In Section 2, we outline our algorithm. Numerical simulation results are provided in Section 3. This is followed by experimental results on IBM quantum (IBMQ) devices in Section 4. Conclusion and some possible future directions are provided in Section 5.

2 Method

A quantum state of d dimension is defined by the density matrix $\rho = \sum_{i=1}^{d} p_i |\psi_i\rangle \langle \psi_i|$ where p_i 's are the ordered probabilities (eigenvalues) such that $0 \leq p_d \leq \ldots \leq p_2 \leq p_1 \leq 1$ and $\sum_{i=1}^{d} p_i = 1$. Let r be the rank of the density matrix ρ . Then, $p_{r+1} = p_{r+2} = \ldots = p_d = 0$. To extract the information from a quantum system, we need to perform the measurements. The outcomes of the measurement follow the probability distribution $\{P_i\}_i$, which is characterized through the Born's rule [4]

$$P_{i} = \operatorname{tr}(|\phi_{i}\rangle\langle\phi_{i}|\rho) = \langle\phi_{i}|\rho|\phi_{i}\rangle. \tag{1}$$

The elementary measurement operators are the collection of positive operators, which sums to the identity operator $\sum_{i} |\phi_{i}\rangle \langle \phi_{i}| = I$ in the d-dimensional Hilbert space.

The SPSA is a stochastic algorithm to obtain the minimum solution of differential equations. In our case, the roots are the eigenvectors $|\psi_i\rangle$ of the density matrix ρ . To sequentially estimate the eigenvectors (eigenstates) of ρ , we design the SPSA to tackle the following optimization problem:

$$\operatorname{arg\,max}_{|\phi\rangle} \quad \langle \phi | \rho | \phi \rangle \\
\operatorname{subject to} \quad \operatorname{tr}(|\phi\rangle \langle \phi|) = 1 \\
|\phi\rangle \langle \phi| \ge 0, \tag{2}$$

which enables to estimate the most dominant eigenvector $|\psi_1\rangle$ of ρ corresponding to the largest eigenvalue p_1 . We provide a sketch of our algorithm to estimate the density matrix ρ of a mixed quantum state (see Figure 1).

(S1) Initialize the learning state vector $|\phi_0\rangle$ to estimate the first eigenvector $|\psi_1\rangle$: Let (d+1) bases $\{|\omega_{ij}\rangle\}_{j=1}^d$, $i=1,2,\ldots,d+1$, be mutually unbiased (MU), enabling to optimally determine the density matrix ρ of an ensemble of d dimensional systems with informational completeness [24, 25]. Since these MU bases have the equal inner-product property across all mutual sets such that $|\langle \omega_{ij} | \omega_{kl} \rangle|^2 = 1/d$ for all $i \neq k, j, l, 1$ we divide the (hyper)space of quantum states into d(d+1) regions of basis states $|\omega_{ij}\rangle$ in the MU bases to initialize the learning state vector $|\phi_0\rangle$. We first form the initializing set $\mathcal{B}_1 = \{|\omega_{ij}\rangle\}$, then measure the density matrix ρ in all the complete

¹See [24] for a construction of complete sets of MU bases.

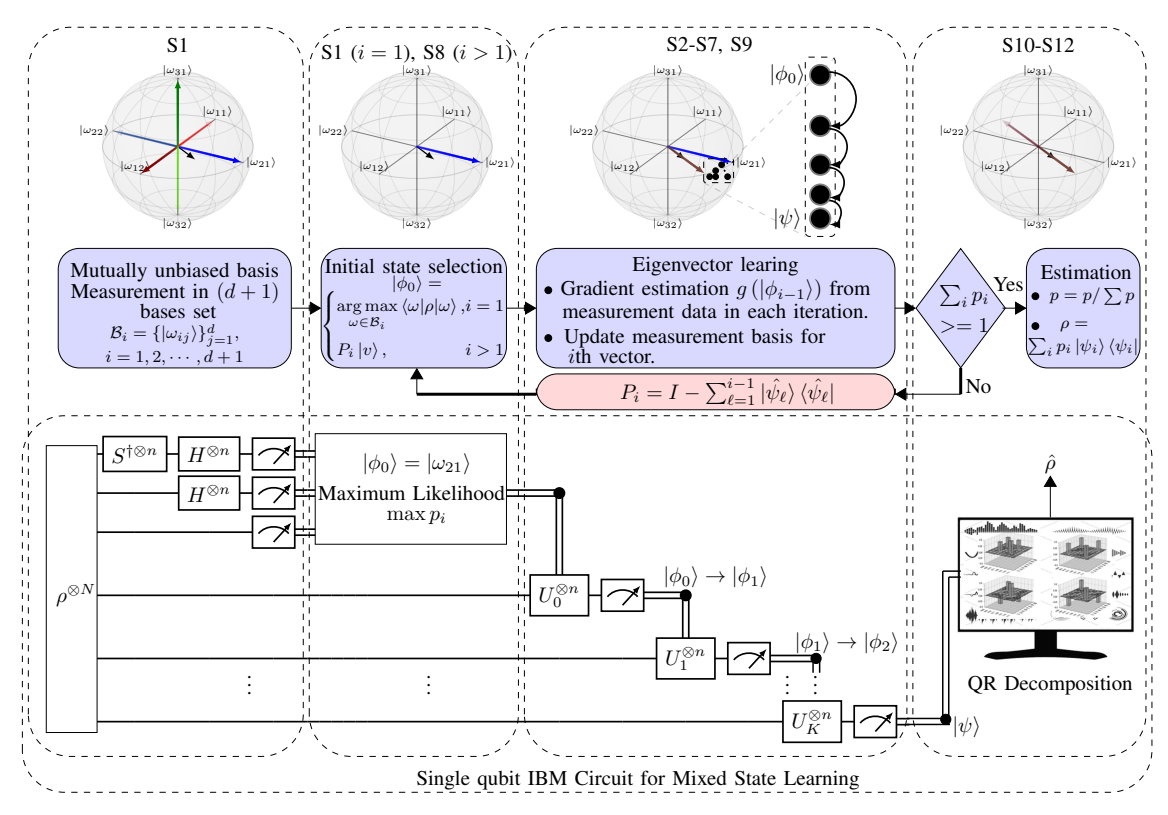


Figure 1: Self-guided quantum state learning for mixed states: The upper panel shows the general working of our algorithm. The state vectors (blue, green, and red) of MU basis and the unknown state (black) are shown in the Bloch sphere in S1. For estimating the first eigenvector (i = 1), the initial state vector $|\phi_0\rangle$ is selected from the basis state that has the maximum expectation on the unknown quantum state. This initial choice is followed by K iterations of stochastic gradient estimation and state update. For estimating the remaining eigenvectors (i > 1), the initial choice is a random vector in the intersection of nullspace of previously estimated eigenvectors. Finally, the obtained probabilities are normalized and the estimate $\hat{\rho}$ is produced. See Section 2 for details. The lower panel shows the quantum circuit for implementation of our algorithm. See Section 4 for details.

d(d+1) MU projectors $|\omega_{ij}\rangle\langle\omega_{ij}|$, and choose the basis state with the maximum probability as the starting state vector $|\phi_0\rangle$ to learn the first eigenvector $|\psi_1\rangle$ as follows:

$$|\phi_0\rangle = \underset{|\omega\rangle \in \mathcal{B}_1}{\arg\max} \langle \omega | \rho | \omega \rangle,$$
 (3)

which is determined by performing N measurements for each projector. Initialize the learning eigenvalue as $q_0 = 0$.

(S2) Set a random vector $\boldsymbol{\delta}_k$ of dimension d whose entries are obtained from the set $\{\pm 1 \pm \sqrt{-1}\}$ with equal probabilities for the kth iteration $(k=1,2,\ldots)$ and use the two gain parameters [22, 26]:

$$\alpha_k = \frac{1}{k^{0.602}}$$

$$\beta_k = \frac{0.1}{k^{0.101}}.$$
(4)

$$\beta_k = \frac{0.1}{k^{0.101}}.\tag{5}$$

(S3) Form two sets $S_k^{\pm} = \left\{ \left| \eta_k^{\pm} \right\rangle \left\langle \eta_k^{\pm} \right|, I - \left| \eta_k^{\pm} \right\rangle \left\langle \eta_k^{\pm} \right| \right\}$ of measurement operators for the kth

iteration where

$$|\eta_k^{\pm}\rangle = \frac{\mathbf{x}_k^{\pm}}{\|\mathbf{x}_k^{\pm}\|},\tag{6}$$

$$\mathbf{x}_k^{\pm} = |\phi_{k-1}\rangle \pm \beta_k \boldsymbol{\delta}_k. \tag{7}$$

(S4) Obtain the gradient vector in the direction of $\boldsymbol{\delta}_k$ as follows:

$$\mathbf{g}(|\phi_{k-1}\rangle) = \left(\frac{\mu_k^+ - \mu_k^-}{2\beta_k}\right) \boldsymbol{\delta}_k \tag{8}$$

where

$$\mu_k^{\pm} = \langle \eta_k^{\pm} | \rho | \eta_k^{\pm} \rangle, \tag{9}$$

which is estimated by performing N measurements for each projector.

(S5) Update the unit-norm learning vector and the learning eigenvalue as follows:

$$|\phi_k\rangle = \frac{\mathbf{y}_k}{\|\mathbf{y}_k\|},\tag{10}$$

$$\mathbf{y}_k = |\phi_{k-1}\rangle + \alpha_k \mathbf{g}\left(|\phi_{k-1}\rangle\right),\tag{11}$$

$$q_k = q_{k-1} + \langle \eta_k^+ | \rho | \eta_k^+ \rangle + \langle \eta_k^- | \rho | \eta_k^- \rangle.$$
 (12)

- (S6) Repeat the steps (S2)-(S5) up to k=K. The updated learning vector produces the estimate $|\hat{\psi}_1\rangle = |\phi_K\rangle$ of the first eigenvector corresponding to the largest eigenvalue of ρ , which converges to $|\psi_1\rangle$ as $K \to \infty$.
- (S7) Obtain the estimate $\hat{p}_1 = q_K/(2K)$ of the largest eigenvalue using a sample average approximation.
- (S8) Initialize the learning state vector $|\phi_0\rangle$ to estimate the *i*th eigenvector $|\psi_i\rangle$, $i \geq 2$: We generate any random vector $|v\rangle$ and select its projection on the intersection of nullspaces of previously estimated eigenvectors, i.e,

$$|\phi_0\rangle = P_i |v\rangle, \tag{13}$$

where $P_i = I - \sum_{\ell=1}^{i-1} |\hat{\psi}_{\ell}\rangle \langle \hat{\psi}_{\ell}|$ is the projector on the nullspace of already estimated eigenstates.

(S9) Refine the quantity μ_k^{\pm} in (9) as

$$\mu_k^{\pm} = \langle \eta_k^{\pm} | \rho | \eta_k^{\pm} \rangle - \sum_{j=1}^{i-1} \left| \langle \eta_k^{\pm} | \hat{\psi}_j \rangle \right|^2$$
 (14)

and iterate the steps (S2)–(S7) to get $|\hat{\psi}_i\rangle$ and \hat{p}_i for $i \geq 2$.

(S10) Stop learning a new eigenvector if the estimated eigenvalues sum up near to one such that $\sum_{i=1}^{\hat{r}} \hat{p}_i \leq 1 - \epsilon$ where \hat{r} is the total number of nonzero estimated eigenvalues, i.e., the estimated rank.

Algorithm 1: Self-guided quantum state learning for mixed states

```
Input: Initializing set \mathcal{B}_1 of MU bases and N_{\max} copies of the density matrix \rho
        Output: Estimated density matrix \hat{\rho}
  i \leftarrow 1
      while i \leq d do
  \mathbf{2}
  3
                 if i = 1 then
                       |\phi_0\rangle \leftarrow \arg\max_{|\omega\rangle \in \mathcal{B}_1} \langle \omega | \rho | \omega \rangle : N measurements for each projector
  5
                         P_{i} \leftarrow I - \sum_{\ell=1}^{i-1} |\hat{\psi}_{\ell}\rangle \langle \hat{\psi}_{\ell}| 
 |\phi_{0}\rangle \leftarrow P_{i} |v\rangle
   6
  7
  8
  9
                 for k \in 1 \to K do
                          Construct vector \boldsymbol{\delta}_k whose entries are chosen randomly from the set \{\pm 1 \pm \sqrt{-1}\}
10
11
                           \alpha_k \leftarrow \frac{1}{k^{0.602}}
                          \beta_k \leftarrow \frac{6.1}{k^{0.101}} \\ |\eta_k^{\pm}\rangle \leftarrow \text{normalized } |\phi_{k-1}\rangle \pm \beta_k \boldsymbol{\delta}_k
13
                          \mu_k^{\pm} \leftarrow \langle \eta_k^{\pm} | \rho | \eta_k^{\pm} \rangle - \sum_{j=1}^{i-1} \left| \langle \eta_k^{\pm} | \hat{\psi}_j \rangle \right|^2 : N measurements for each projector
                         \mathbf{g}(|\phi_{k-1}\rangle) \leftarrow \left(\frac{\mu_k^+ - \mu_k^-}{2\beta_k}\right) \boldsymbol{\delta}_k
15
                          |\phi_k\rangle \leftarrow \text{normalized } |\phi_{k-1}\rangle + \alpha_k \mathbf{g}(|\phi_{k-1}\rangle)
16
                     q_k \leftarrow q_{k-1} + \langle \eta_k^+ | \rho | \eta_k^+ \rangle + \langle \eta_k^- | \rho | \eta_k^- \rangle
17
                 |\hat{\psi}_i\rangle \leftarrow |\phi_K\rangle
18
                 \begin{array}{l} \hat{p}_i \leftarrow \frac{1}{2K} q_K \\ \hat{r} \leftarrow i \end{array}
19
20
                 if \sum_{j=1}^{i} \hat{p}_{j} \leq 1 - \epsilon then i \leftarrow i+1
21
22
                  else
23
                   i \leftarrow d+1
        \begin{bmatrix} |\hat{\psi}_1^*\rangle & |\hat{\psi}_2^*\rangle & \cdots & |\hat{\psi}_{\hat{r}}^*\rangle \end{bmatrix} \leftarrow \operatorname{qr}(\begin{bmatrix} |\hat{\psi}_1\rangle & |\hat{\psi}_2\rangle & \cdots & |\hat{\psi}_{\hat{r}}\rangle \end{bmatrix})
       if \hat{r} = d then
                 for i \in 1 \to \hat{r} do
27
                   \hat{p}_i^* \leftarrow \hat{p}_i
28
                \hat{p}_i^* \leftarrow \hat{p}_i^* / \sum_i \hat{p}_i^*
29
30 else
                for i \in 1 \to \hat{r} do
31
                  \hat{p}_{i}^{*} \leftarrow \langle \hat{\psi}_{i}^{*} | \rho | \hat{\psi}_{i}^{*} \rangle : 2NK(d - \hat{r}) \text{ measurement in } \mathcal{B}_{\hat{\rho}}
33 return \hat{\rho} \leftarrow \sum_{i=1}^{\hat{r}} \hat{p}_i^* \ket{\hat{\psi}_i^*} \bra{\hat{\psi}_i^*}
```

(S11) Form the orthonormal basis

$$\mathcal{B}_{\hat{\rho}} = \left\{ |\hat{\psi}_i^*\rangle \mid i = 1, 2, \dots, \hat{r} \right\}$$
 (15)

using the Gram-Schmidt process with the estimated eigenvectors $|\hat{\psi}_1\rangle$, $|\hat{\psi}_2\rangle$, ..., $|\hat{\psi}_{\hat{r}}\rangle$. Set the estimated eigenvalues to $\hat{p}_i^* = \hat{p}_i$ if $\hat{r} = d$ (full rank) and normalize them. Otherwise, estimate the eigenvalues $\{\hat{p}_i^*\}_i$ by measuring the remaining $2NK(d-\hat{r})$ copies of the quantum state in $\mathcal{B}_{\hat{\rho}}$.

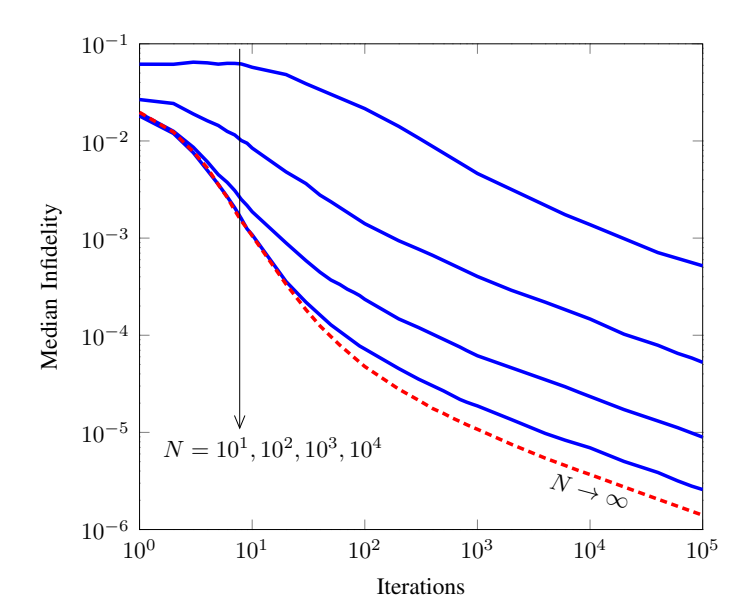


Figure 2: The median infidelity against the number of iterations achieved by our algorithm. Each blue line shows the median performance of the 10^3 randomly generated qubit states according to the Haar measure. The repetitions per measurement setting are $N=10^1,10^2,10^3$, and 10^4 . The red dashed line shows the asymptotic performance, i.e., $N\to\infty$.

(S12) Construct finally the density matrix as follows:

$$\hat{\rho} = \sum_{i=1}^{\hat{r}} \hat{p}_i^* |\hat{\psi}_i^*\rangle \langle \hat{\psi}_i^*|. \tag{16}$$

The pseudocode of self-guided for mixed state is given in Algorithm 1, which utilizes $N_{\rm tot} = N\left(d\left(2K+1\right)+1\right)$ copies of the d-dimensional unknown state ρ .

3 Results

First, we compare the computational complexity of our post-processing step with the post-processing in other well known quantum state tomography methods. The computational complexity of our algorithm is $O(d^3)$, which is due to the Gram-Schmidt decomposition [27]. Since we only need to store estimated eigenvectors, the storage space requirement for our algorithm is $O(\hat{r}d)$. In comparison, the standard quantum tomography has the computational complexity $O(12^n)$ for estimating an d-qubit state [28, 29]. While SGQT offers excellent advantage in the computational complexity, i.e., no post-processing is required, it is only applicable for the tomography of pure states. The hybrid model PAQT is applicable on general (mixed) quantum states at the cost of increased computational complexity and storage space of the system. Its computational cost depends on the Bayesian mean estimation. Bayesian mean estimation with particle filtering requires computational cost $O(d^4Mp)$ for a $d \times d$ state where M is the number of measurements and p is the number of particles. Its storage space requirement is also large since it requires storing all the particles, i.e., elements in $\mathbb{C}^{d \times d}$.

To ascertain the accuracy and effectiveness of our procedure, we use infidelity as a figure of merit. The infidelity between the density matrix ρ and its estimate $\hat{\rho}$ is defined as [4]

$$\bar{F}(\rho,\hat{\rho}) = 1 - \left(\operatorname{tr}\sqrt{\sqrt{\rho}\hat{\rho}\sqrt{\rho}}\right)^2$$
 (17)

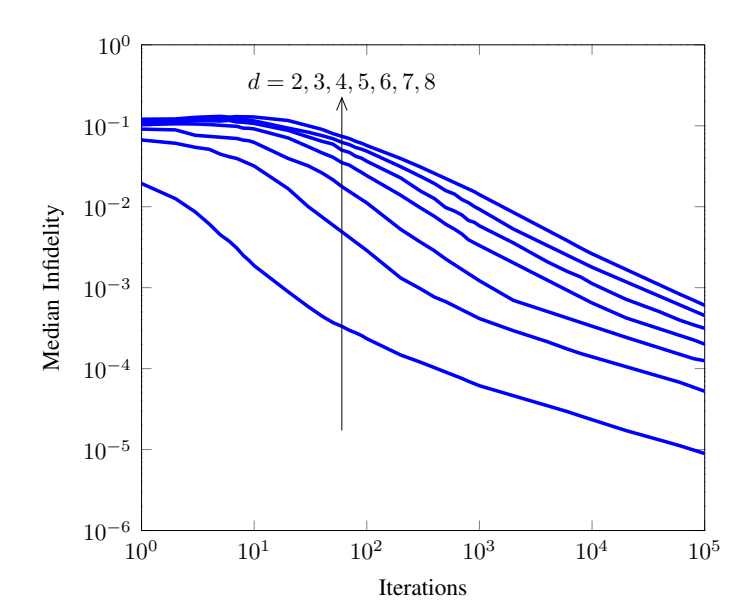


Figure 3: The median infidelity against the number of iterations achieved through our algorithm for qudit $(d \ge 2)$ states. We have fixed the number of measurements per iteration $N=10^3$. Each line is the median performance of our procedure over 10^2 randomly generated mixed states according to the Haar measure.

and its median value over the ensemble of the density matrix ρ is denoted by $\bar{F}_{\rm med}(\rho,\hat{\rho})$. Instead of the mean infidelity, we use the median infidelity due to its robust statistical nature that is not skewed by relatively few outliers in the estimation. We set $\epsilon = 10^{-4}$ for all examples.

Figure 2 shows the median infidelity $\bar{F}_{\rm med}(\rho,\hat{\rho})$ as a function of the iteration number K when the measurement repetitions are set to $N=10^1,10^2,10^3$ and 10^4 , where 10^3 mixed qubit states (d=2) are generated at random according to the Haar measure. For comparison, we also plot the asymptotic infidelity as $N\to\infty$ (red dashed line). We can clearly see the infidelity is improving as we increase the number of iterations along with the number of measurements per iteration.

In Figure 3, we plot the median infidelity of the mixed states estimated via our technique for d = 2, 3, 4, 5, 6, 7, 8 against the number of iterations where we have fixed the number of measurements per iteration $N = 10^3$. As expected, we require more copies to achieve a given infidelity for higher dimensional mixed quantum states.

Another feature of our protocol is its robustness against channel and measurement noise. To demonstrate this robustness, we perform noisy execution of our algorithm where we introduce uniform random noise in the measurement outcomes. To this end, we multiply the obtained vector of estimated probabilities with a doubly stochastic matrix Λ , which is equivalent to employing a faulty measurement device [30, 31]. The elements of Λ are

$$\Lambda_{i,j} = \begin{cases} 1 - \lambda + \lambda/d, & \text{when } i = j\\ \lambda/d, & \text{otherwise,} \end{cases}$$

where λ controls the strength of introduced noise in the measurement outcomes. A noiseless measurement device corresponds to $\lambda = 0$, and a completely random measurement device has $\lambda = 1$. This particular measurement can also be modeled as a depolarizing noise on the state before measurement, followed by a noiseless measurement device [32].

In Figure 4, we plot the ideal performance of our algorithm as well as its performance with measurement (equivalently, depolarizing) noise with $\lambda = 0.2$. For comparison, we

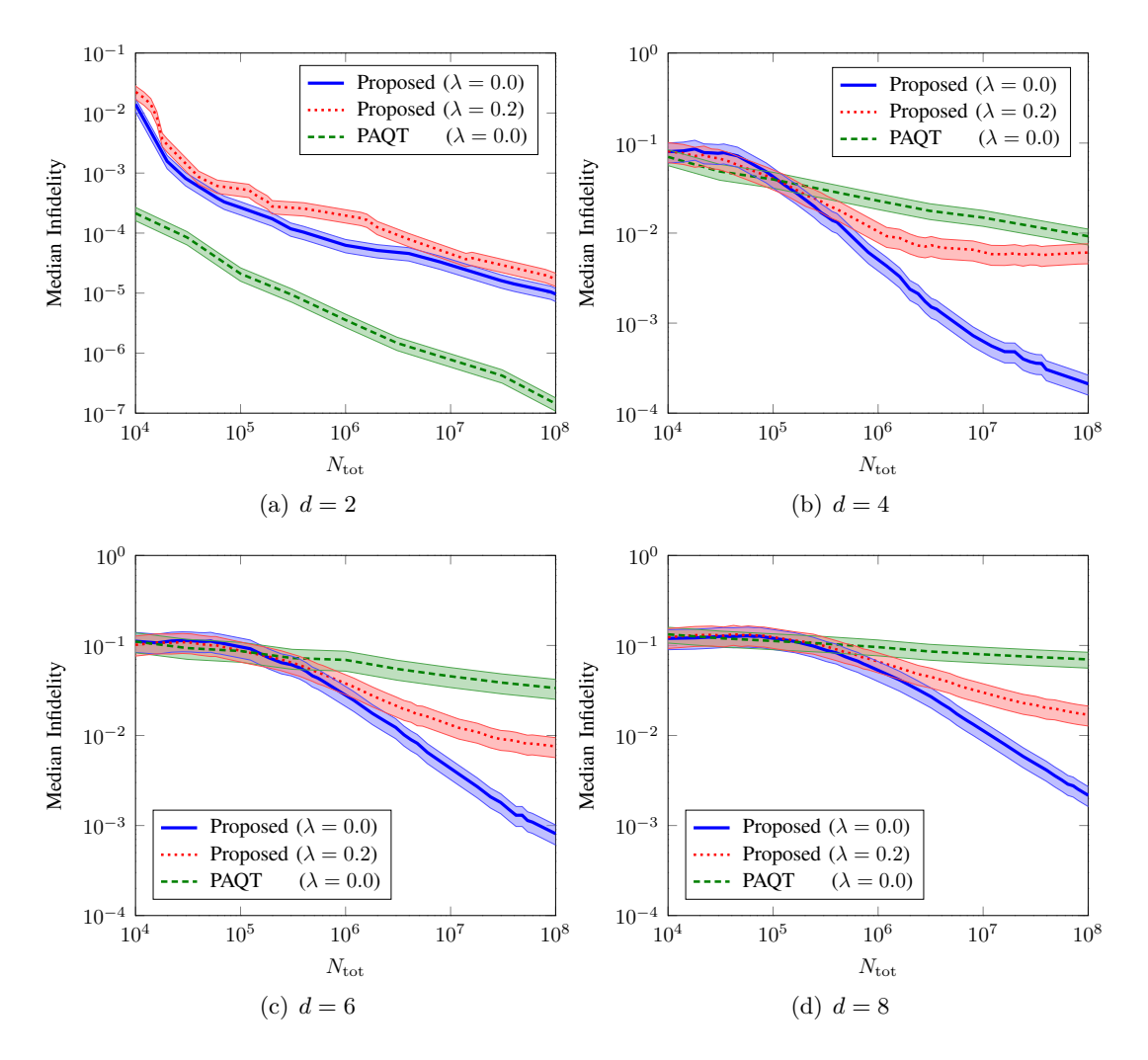


Figure 4: The median infidelity against the number of copies achieved by proposed scheme and PAQT with measurement noise of strength λ . Each line is the median performance over 100 randomly generated quantum states according to the Haar measure. For our algorithm, we utilize 10^4 copies for MU bases measurement of S1. Then, we fix $N=10^3$, and $K=\left(N_{\rm tot}-10^4\right)/Nd$ such that the total copies are same for all d. For PAQT, we use $N=10^3$, $K=10^5$, resampling parameter a=0.9, and number of particles $p=2000,\ 32000,\ 64000,\ and\ 96000$ for d=2,4,6, and 8, respectively. The shaded regions represent 25-75% quantiles of our data.

also plot the noiseless performance of PAQT. Since the type of noise (depolarizing) we introduce in our system pushes the eigenvalues of the estimated state to 1/d, the largest eigenvalue of the noiseless state cannot be smaller than the estimated largest eigenvalue. For this reason, we omit the first estimated eigenvalue from the normalization step. That is, let $S = \sum_i \hat{\lambda}_i$, we normalize the set of eigenvalues as $\lambda_1^* = \hat{\lambda}_1$, and $\lambda_i^* = \hat{\lambda}_i/S$ for $1 < i \le t$, where t is the largest number such that $\sum_{i=1}^t \lambda_i^* \le 1$. There are two key insights from the analysis of Figure 4. First, the relative advantage of our algorithm over PAQT becomes more pronounced as we increase the dimension d of the quantum state. Second, the proposed scheme continues to outperform noiseless PAQT for higher d, even when a uniform noise of moderate strength $\lambda = 0.2$ is introduced in our algorithm.

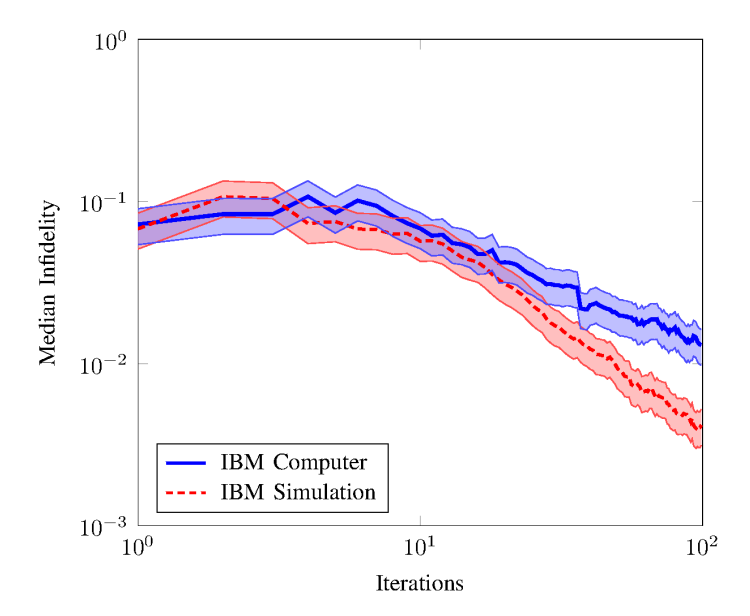


Figure 5: The median infidelity vs the number of iterations achieved by proposed algorithm on IBMQ device and Simulator. Both lines represent the median infidelity over 50 randomly generated mixed states according to the Haar measure. The shaded region represents 25% quantile over the trials. We used 100 shots per iteration.

4 Experimental Results

We experimentally demonstrate our algorithm on IBMQ devices [33]. We have run our experiments on ibmqx2 processor that has average CNOT and readout errors of $1.577e^{-2}$ and $4.538e^{-2}$, respectively.

In order to prepare mixed qubit states on the IBMQ devices, we prepare a purification on two qubits of the intended state followed by the tomography on only one of the qubits. The purification of a density matrix ρ^A that has the eigendecomposition $\sum_i p_i |\psi_i\rangle \langle \psi_i|$ is given by the composite system

$$|\psi\rangle_{AR} = \sum_{i} \sqrt{p_i} |\psi_i\rangle_A \otimes |r_i\rangle_R,$$
 (18)

where $|r_i\rangle_R$ is an orthonormal basis of the reference system R. Then, the original mixed state is related with the composite system as

$$\rho^{A} = \operatorname{tr}_{R}(|\psi\rangle_{AR}\langle\psi|_{AR}). \tag{19}$$

For our algorithm, the bases are changing in each iteration. To measure the quantum state in desired basis, we apply unitary on the given quantum state. The lower panel in Figure 1 shows the circuit that we implemented on the IBMQ device where

$$H = \frac{1}{\sqrt{2}} \begin{bmatrix} 1 & 1\\ 1 & -1 \end{bmatrix}, \qquad S^{\dagger} = \begin{bmatrix} 1 & 0\\ 0 & e^{-\frac{i\pi}{2}} \end{bmatrix}, \tag{20}$$

and the unitary U_i is the general unitary denoted by u3 in the IBMQ programming framework. Its expression is given by

$$u3(\theta, \phi, \lambda) = \begin{bmatrix} \cos\left(\frac{\theta}{2}\right) & -e^{i\lambda}\sin\left(\frac{\theta}{2}\right) \\ e^{i\phi}\sin\left(\frac{\theta}{2}\right) & e^{i(\phi+\lambda)}\cos\left(\frac{\theta}{2}\right) \end{bmatrix}, \tag{21}$$

where θ , ϕ and λ are determined by orthonormal basis in which we want to measure the state

Figure 5 shows the performance of our algorithm on IBM computer and IBM simulator. IBM computer performance deviates from the simulator due to the state preparation, gate, and measurement errors in the device.

5 Conclusion

We have provided an online learning algorithm for quantum state tomography. Our algorithm features iterative applications of SPSA for resource efficient and accurate estimates of an unknown quantum state in higher dimensions. Numerical examples demonstrate the better performance as compared to the contemporary online learning algorithms. In particular, our proposal demonstrates a better robustness against measurement noise, which makes it suitable for near-term applications. Future works may include photonic implementations of the proposed algorithm to further analyze its practical advantages. In addition, our proposed algorithm can be utilized for efficient approximate eigendecomposition of Hermitian matrices.

Acknowledgments

This work was upheld by the National Research Foundation of Korea (NRF) give financed by the Korea government (MSIT) (No. 2019R1A2C2007037)

References

- [1] Nicolas Gisin and Rob Thew. Quantum communication. *Nat. Photon.*, 1(3):165–171, March 2007. DOI: https://doi.org/10.1038/nphoton.2007.22.
- [2] H.-J. Briegel, W. Dur, J. I. Cirac, and P. Zoller. Quantum repeaters: The role of imperfect local operations in quantum communication. *Phys. Rev. Lett.*, 81:5932–5935, December 1998. DOI: 10.1103/PhysRevLett.81.5932.
- [3] David P DiVincenzo. Quantum computation. Science, 270(5234):255–261, October 1995. DOI: 10.1126/science.270.5234.255.
- [4] Michael A Nielsen and Isaac Chuang. Quantum computation and quantum information, April 2002.
- [5] Vittorio Giovannetti, Seth Lloyd, and Lorenzo Maccone. Advances in quantum metrology. *Nat. Photon.*, 5(4):222, March 2011. DOI: https://doi.org/10.1038/nphoton.2011.35.
- [6] C. L. Degen, F. Reinhard, and P. Cappellaro. Quantum sensing. Rev. Mod. Phys., 89 (3):1–39, July 2017. DOI: 10.1103/RevModPhys.89.035002.
- [7] T. Opatrný, D.-G. Welsch, and W. Vogel. Least-squares inversion for density-matrix reconstruction. *Phys. Rev. A*, 56:1788–1799, September 1997. DOI: 10.1103/Phys-RevA.56.1788.
- [8] K. Banaszek, G. M. D'Ariano, M. G. A. Paris, and M. F. Sacchi. Maximum-likelihood estimation of the density matrix. *Phys. Rev. A*, 61:010304, December 1999. DOI: 10.1103/PhysRevA.61.010304.
- [9] Yong Siah Teo, Huangjun Zhu, Berthold-Georg Englert, Jaroslav Reháček, and Zdenék Hradil. Quantum-state reconstruction by maximizing likelihood and entropy. *Phys. Rev. Lett.*, 107:020404, July 2011. DOI: 10.1103/PhysRevLett.107.020404.

- [10] Robin Blume-Kohout. Hedged maximum likelihood quantum state estimation. *Phys. Rev. Lett.*, 105(20):200504, November 2010. DOI: 10.1103/PhysRevLett.105.200504.
- [11] Robin Blume-Kohout. Optimal, reliable estimation of quantum states. New J. Phys., 12(4):043034, April 2010. DOI: 10.1088/1367-2630/12/4/043034.
- [12] Christopher Granade, Joshua Combes, and D G Cory. Practical Bayesian tomography. *New J. Phys.*, 18(3):033024, March 2016. DOI: 10.1088/1367-2630/18/3/033024.
- [13] F. Huszár and N. M. T. Houlsby. Adaptive Bayesian quantum tomography. *Phys. Rev. A*, 85:052120, May 2012. DOI: 10.1103/PhysRevA.85.052120.
- [14] K. S. Kravtsov, S. S. Straupe, I. V. Radchenko, N. M. T. Houlsby, F. Huszár, and S. P. Kulik. Experimental adaptive Bayesian tomography. *Phys. Rev. A*, 87:062122, June 2013. DOI: 10.1103/PhysRevA.87.062122.
- [15] Bo Qi, Zhibo Hou, Li Li, Daoy Dongi, Guoyong Xiang, and Guangcan Guo. Quantum state tomography via linear regression estimation. *Sci. Rep.*, 3:3496, December 2013. DOI: 10.1038/srep03496.
- [16] Bo Qi, Zhibo Hou, Yuanlong Wang, Daoyi Dong, Han-Sen Zhong, Li Li, Guo-Yong Xiang, Howard M Wiseman, Chuan-Feng Li, and Guang-Can Guo. Adaptive quantum state tomography via linear regression estimation: Theory and two-qubit experiment. npj Quantum Inf., 3(1):1–7, April 2017. DOI: 10.1038/s41534-017-0016-4.
- [17] Christopher Ferrie. Self-guided quantum tomography. *Phys. Rev. Lett.*, 113:190404, November 2014. DOI: 10.1103/PhysRevLett.113.190404.
- [18] Robert J. Chapman, Christopher Ferrie, and Alberto Peruzzo. Experimental demonstration of self-guided quantum tomography. *Phys. Rev. Lett.*, 117:040402, July 2016. DOI: 10.1103/PhysRevLett.117.040402.
- [19] Christopher Granade, Christopher Ferrie, and Steven T Flammia. Practical adaptive quantum tomography. New J. Phys., 19(11):113017, November 2017. DOI: 10.1088/1367-2630/aa8fe6.
- [20] Abhijeet Melkani, Clemens Gneiting, and Franco Nori. Eigenstate extraction with neural-network tomography. *Phys. Rev. A*, 102:022412, August 2020. DOI: 10.1103/PhysRevA.102.022412.
- [21] Markus Rambach, Mahdi Qaryan, Michael Kewming, Christopher Ferrie, Andrew G. White, and Jacquiline Romero. Robust and efficient high-dimensional quantum state tomography. *Phys. Rev. Lett.*, 126:100402, March 2021. DOI: 10.1103/Phys-RevLett.126.100402.
- [22] A Utreras-Alarcón, M Rivera-Tapia, S Niklitschek, and A Delgado. Stochastic optimization on complex variables and pure-state quantum tomography. Sci. Rep., 9(1): 1–7, November 2019. DOI: 10.1038/s41598-019-52289-0.
- [23] J. C. Spall. Multivariate stochastic approximation using a simultaneous perturbation gradient approximation. *IEEE Trans. Automat. Contr.*, 37(3):332–341, March 1992. DOI: 10.1109/9.119632.
- [24] William K Wootters and Brian D Fields. Optimal state-determination by mutually unbiased measurements. *Ann. Phys.*, 191(2):363 381, October 1989. ISSN 0003-4916. DOI: https://doi.org/10.1016/0003-4916(89)90322-9.
- [25] Junaid ur Rehman, Ahmad Farooq, and Hyundong Shin. Discrete Weyl channels with Markovian memory. *IEEE J. Sel. Areas Commun.*, 38(3):413–426, March 2020. DOI: DOI: 10.1109/JSAC.2020.2968993.
- [26] P. Sadegh and J. C. Spall. Optimal random perturbations for stochastic approximation using a simultaneous perturbation gradient approximation. *IEEE Trans. Automat.* Contr., 43(10):1480–1484, October 1998. DOI: 10.1109/9.720513.

- [27] Åke Björck. Solving linear least squares problems by Gram-Schmidt orthogonalization. BIT Numer. Math., 7(1):1–21, 1967. DOI: https://doi.org/10.1007/BF01934122.
- [28] Zhibo Hou, Han-Sen Zhong, Ye Tian, Daoyi Dong, Bo Qi, Li Li, Yuanlong Wang, Franco Nori, Guo-Yong Xiang, Chuan-Feng Li, and Guang-Can Guo. Full reconstruction of a 14-qubit state within four hours. New J. Phys., 18(8):083036, August 2016. DOI: 10.1088/1367-2630/18/8/083036.
- [29] John A. Smolin, Jay M. Gambetta, and Graeme Smith. Efficient method for computing the maximum-likelihood quantum state from measurements with additive gaussian noise. *Phys. Rev. Lett.*, 108:070502, February 2012. DOI: 10.1103/Phys-RevLett.108.070502.
- [30] Filip B. Maciejewski, Zoltán Zimborás, and Michał Oszmaniec. Mitigation of readout noise in near-term quantum devices by classical post-processing based on detector tomography. *Quantum*, 4:257, April 2020. DOI: 10.22331/q-2020-04-24-257.
- [31] Muhammad Asad Ullah, Junaid ur Rehman, and Hyundong Shin. Quantum frequency synchronization of distant clock oscillators. *Quantum Inf. Process.*, 19(5):144, May 2020. ISSN 1573-1332. DOI: 10.1007/s11128-020-02644-2.
- [32] Junaid ur Rehman and Hyundong Shin. Entanglement-free parameter estimation of generalized Pauli channels, February 2021.
- [33] 5-qubit backend: IBM Q team, IBM Q 5 ibmqx5 backend specification v2.2.7. (Accessed: Feb 2021).